The Influence of Spatial Heterogeneity and Material Characteristics on Fluid Flow Patterns Through Two Unsaturated, Mixed Waste-rock Piles.

Sharon Blackmore[1], Brad Speidel[2], Andrew Critchley[3], Roger D. Beckie[4], K. Ulrich Mayer[5], Leslie Smith[6]

[1,2,3,4,5,6] Department of Earth and Ocean Sciences, University of British Columbia, Vancouver, BC, Canada;
[1](sblackmore@eos.ubc.ca), [2](brspeidel@gmail.com), [3](ACritchley@bgcengineering.ca), [4](rbeckie@eos.ubc.ca),
[5](umayer@eos.ubc.ca), [6](lsmith@eos.ubc.ca)

.

Abstract

A tracer study was performed on five experimental waste-rock piles at the Antamina mine (Peru) to investigate the effect of material characteristics on pile hydrology. This paper focuses on two heterogeneous piles: Pile 4, a coarse-grained pile with alternating carbonate-rich Class C and moderately reactive Class B material; and Pile 5, containing alternating Class C material and reactive, finer-grained Class A material. Initial breakthrough from Pile 4 was observed within hours of tracer release and half the applied mass was recovered within one month. Pile 5 breakthrough was slower and with significantly lower concentrations. Tracer concentrations and release rates characterize varied flow regimes for the three material classes. Low tracer concentrations and slower release rates suggest matrix flow within Class A-rich regions. Conversely, rapid tracer release and high initial tracer concentrations indicates a significant component of preferential flow within Class C material. Class B-rich regions provide evidence of preferential and matrix flow. Physical material characteristics support these trends, with Class A having high air-entry values, with considerably lower values for Class B/C material. Internal pile geometry and varied unsaturated hydraulic conductivities, from alternating waste-rock layers, promote a horizontal flow component, which may decrease rock-water interaction times through finer-grained, reactive material.

Key Words: Antamina, NRD, bromide, macropore, preferential flow, matrix.

1. Introduction

The Antamina mine, located 270 km northeast of Lima, is a large polymetallic skarn deposit. Open pit mining techniques, such as those used at Antamina, cannot avoid the production of large amounts of waste-rock and greater than 2.2 billion tonnes of waste-rock is expected to be produced under the current mine plan. The understanding of water infiltration and drainage through Antamina's waste-rock dumps is important for the assessment and prediction of drainage quality. Additionally, the geochemistry of Antamina's waste-rock (i.e., carbonate-hosted sulphides) makes it a site of interest to investigate neutral rock drainage (NRD) conditions, due to coupled sulphide oxidation (acid-generation) and carbonate dissolution (acid-consumption) processes.

Previous work by Bay (2009) highlights a strong hydrological control on sulphide oxidation and mineral weathering at the Antamina site. The unsaturated nature of waste-rock piles at Antamina and its location in a distinct wet and dry season climate (annual precipitation ~ 1400 mm) provide significant opportunity for both infiltration and mineral weathering. Clast-size heterogeneity of waste-rock, due to blasting or excavation, may range over 6 orders of magnitude and can strongly influence infiltration (e.g., 1 µm – 1 m; Nichol et al., 2005; Fala et al., 2005).

Waste-rock with a large proportion of fine material behaves in a 'soil-like' manner. This type of infiltration results in dominantly matrix flow, high water residence times, and increased rates of sulphide weathering and metal release (Aubertin et al., 2003; Fala et al., 2005, Smith and Beckie, 2003, Sracek et al., 2004). Conversely, waste-rock containing a high proportion of coarser-grained material behaves in a ‘rock-like’ manner (Smith and Beckie, 2003) and infiltration may incorporate a significant component of preferential flow, and reduced residence times (Smith and Beckie, 2003; Aubertin et al., 2003; Fala et al., 2005).

Antamina’s waste-rock is classified into three classes; Class A, B and C (Golder, 2004). Class A is finer grained skarn or intrusive material with higher sulphide and metal percentages. Class B and C have similar geology (i.e., hornfels, marble), with lower sulphide and metal concentrations than Class A and are relatively coarse-grained. Refer to Golder (2010) and Hirsche et al. (2012) for details on the chemical descriptions of the Antamina waste-rock classification scheme.

A tracer study, complementary laboratory tests, and modeling were utilized to examine the influence of waste-rock physical characteristics on hydrological flow regimes from five mesoscale experimental piles. The focus of this paper is on two mixed waste-rock piles (Class B and C, Pile 4; Class A and C, Pile 5), which are small-scale analogs of operating waste-rock piles at Antamina, the Tucush Dump and East Dump (respectively). The goal of this study is to better understand waste-rock hydrology for mixed material, which will assist future considerations of its impact on geochemical processes and subsequent drainage. The outcome of this study may have implications to sites with similar mineral composition or similarly diverse waste-rock material characteristics.

2. Methodology

2.1 Waste-rock pile construction

Pile 4 and 5 (36 m (*l*) x 36 m (*w*) x 10 m (*h*)) were constructed from May 2008 – April 2009, with a crown of ~ 14 m x 24 m and a 37^{o} slope (Figure 1). Four lysimeters constructed with impermeable geomembrane were installed at the base of the pile to capture flow. Three are 4 m x 4 m sub-lysimeters (Lysimeter A – C), which captures flow through a unique combination of Class A/B and Class C material. One large lysimeter (Lysimeter D) captures all flow from the pile’s base, excluding flow through the sub-lysimeters. Each waste-rock pile contains 6 instrumentation lines to continuously measure physical parameters (e.g., temperature, electrical conductivity and volumetric water content) to provide details of wetting front migration. Drainage from all the lysimeters flows to an instrumentation hut, which contains tipping buckets at the terminal flow point to record flow rate and volume. Refer to Bay et al. (2009) for further details and schematics detailing the construction of waste-rock piles at Antamina. Pile 4 consists of 75% (v/v) Class C material (marble – hornfels, non-reactive) and 25 % Class B material (marble, slightly reactive). Pile 5 consists of 52% Class C material and 48% Class A material (intrusive, reactive). Refer to Figure 1 for a schematic of Pile 4 and 5 geometry.

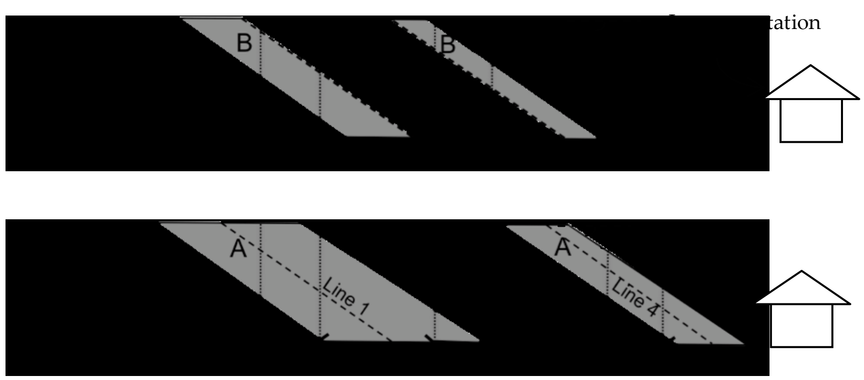

Figure 1. Schematic of Pile 4 and 5 composition and location of lysimeters and instrumentation lines.

2.2 Design and operation of tracer test

Tracers used in the tracer application were selected based on four criteria; (i) natural concentrations of tracers are low to negligible; (ii) tracers are non-toxic to surrounding habitat; (iii) tracers are cost-efficient; and (iv) ability to analyze tracer using an inexpensive, rapid method to produce results quickly and with high-reproducibly. It is estimated that applied tracer concentrations may undergo a maximum of 100 to 1000 times dilution by mixing with resident waters within waste-rock pile porespace and in the basal drainage.

One conservative and one non-conservative tracer were selected for this study. Bromide was selected as the conservative tracer due to its low background concentrations at Antamina (i.e., 0.2 – 0.8 ppm), high stability, low toxicity to flora/fauna, and analyses using spectrophotometry or ion chromatography. No preservation methods are required for bromide due to its high stability. Uranine ($C_{20}H_{10}O_5Na$), a sodium-fluorescein producing a green fluorescence when dissolved in water, was selected as a second tracer due to its ease of detection and negligible background concentrations in waste-rock drainage (0 – 0.5 ppb). Batch experiments using waste rock obtained from Antamina and increasing uranine concentrations indicated this tracer behaves non-conservatively, as per significant adsorption to Class A material and lesser Class B and C material. All uranine samples are analyzed using fluorescent spectophotometry.

The tracers were applied on Pile 4 and 5 on January 23rd and 24th, 2010 (respectively). The tracer solution contained ~ 3000 mg/L bromide (from LiBr) and ~10 mg/L uranine, and was applied on the crown of each pile. Characteristics of the tracer application for each pile are shown in Table 1. The tracer event characteristics corresponded to approximately a 4-year return period event, as per rainfall intensity-duration-frequency curves calculated for Antamina (Golder, 1999). The uniformity of the tracer application was determined by measuring tracer volumes from approximately 90 uniformly placed small-volume collectors on the crown of each pile. The computed Christiansen Uniformity Co-efficient (CUC; Christiansen, 1942) for both Pile 4 and 5 corresponded to a reasonably uniform application. No ponding or surficial runoff occurred during Pile 4 and 5 tracer application.

Table 1. Tracer Application Characteristics.

Pile		Tracer footprint (m^2)	Applied Volume (L)	Duration (hr)	[Uranine] (mg/L)	[Bromide] (mg/L)	CUC
4	B and C	336 m^2	8,829	4.75	9.14	2,900	82
5	A and C	311 m^2	8,354	5.17	11.2	3,046	77

Following tracer application, water samples were collected at terminal flow points from the 4 lysimeters. Sampling frequency varied throughout the tracer study, from frequent (15 – 30 minutes), immediately following tracer application, to intermittent (1 – 2 samples/week). A more intermittent frequency was maintained until the onset of the 2010 wet season (i.e., end of October), when sampling frequency was increased. All samples were dispensed into 15 ml opaque HDPE bottles and kept cool for transport.

2.3 Laboratory analyses

Bromide concentrations from water samples were measured using a spectrophotometric method (Presley, 1971) and measured at an absorbance of $\lambda = 595$ nm. Samples were analyzed for uranine using a Varian® Cary Eclipse fluorescence spectrophotometer (courtesy of the Laboratory of Molecular Biophysics, Spectroscopy and Kinetics Hub, University of British Columbia, Vancouver, BC, Canada). Duplicates were performed every 25 samples for quality assurance and quality control purposes.

Data gaps, due to missed sampling, were interpolated from weekly dissolved lithium concentrations. Specifically, bromide concentrations were derived from a moderately strong (i.e., $r^2 > 0.7$) positive correlation with lithium concentrations in the weeks preceding or succeeding the data gap(s). Uranine concentrations were interpolated in a similar manner, by comparison of bromide to uranine values, and produced moderate to strong correlations (i.e., $r^2 = 0.5 – 0.9$). Inferred tracer concentrations are denoted by dashed lines in succeeding figures.

2.4 Flow rates and loading calculations

Tipping buckets are located at the outflow of drainage from the four lysimeters (A – D) from each pile. Tipping buckets are calibrated once per year to develop a relationship between tip rate and tip volume. Flow rates and cumulative flow volumes are extracted from tip rates recorded from each lysimeter and used to calculate tracer mass loading values. Tracer loadings for each lysimeter were calculated by multiplying the tracer concentration (as mg/m^3) from spectrophotometric methods by the volumetric sum of discharged water from the lysimeter (as m^3/day or m^3/week).

2.5 Material characteristic analyses

Fourteen samples from the three waste-rock classes used in the piles were characterized by three measures; particle size distribution, bulk density, and porosity. The results from these analyses were used in the estimation of the material's soil-water characteristic curve. The methods used in these soil characteristic analyses are described in the following sections.

2.5.1 Particle size distribution (PSD)

PSD analyses followed ASTM standard methodologies (ASTM D 5519-94) and included up to 24 different mesh sizes (i.e., 74 µm – 2.032 m) (Golder, 2010). Each fraction was weighed and plotted in terms of "percent passing" (i.e., $M_{sieve\ fraction}/M_{total} \times 100\%$).

2.5.2 Bulk density and porosity

Bulk density values were determined for Class A and B material and porosity was measured for Class A material only (Golder, 2010). The characteristics for the remaining Class B and Class C were measured at the University of British Columbia. Bulk dry density of Class C material was calculated by drying, weighing and packing material in a container of measurable volume. Porosity measurements for Class B and C material were calculated by slowly saturating the packed material until the water level reached the top of rock volume and it was assumed the porespace was fully occupied.

2.5.3 Soil water characteristic curves

A direct and indirect method was used to determine soil-water characteristic curves (SWCCs) for Antamina waste-rock classes. The SWCC of a material is unique to every soil type and describes the amount of water which will remain in the pore space under applied matric suctions. Two parameters are calculated from SWCCs; the air-entry value and residual saturation. The former is defined as the critical pressure at which air is displaced by water into the material's pore space, whereas the latter is the amount of water that will remain in the pore space following its drainage. Tempe cells were used to directly determine the relationship between soil matric suction and water content (Fredlund et al., 1997). Preparation of the cells followed previous literature (e.g., SoilMoisture Corp, 1995). Only two waste-rock classes were analyzed: Class A-intrusive and Class B material (hornfels), and material limited to particles passing a screen <4.75 mm (Mesh #4). Material was packed onto a 6.39 cm (diameter) ceramic plate to a height of 3.18 cm and subjected to pressures between 1 – 12 kPa, via elevation head differences, and 12 – 100 kPa, by regulated pressure differences.

Soil Vision software (based on Fredlund and Xing, 1994) was used to determine SWCCs using an indirect method combining soil characteristics (e.g., bulk density, porosity, water content, void ratio, specific gravity) and PSD data. For the latter, only material for sieve sizes less than 4 mm were used, as coarser material does not contribute to a soil's capillarity. Using a curve-fitting equation (Fredlund and Xing, 1994), SoilVision assigns an equation to the PSD data points and estimates the percentages of sand, silt and clay for the soil. SoilVision then generates a SWCC by coupling the soil's three known geotechnical characteristics and its fitted PSD data with SoilVision's database of over 6000 soils. SWCC were estimated for all waste-rock classes.

3. Results and Discussion

3.1 Flow characteristics

3.1.1 Pile 4 – Class B and C material

Bromide and uranine concentrations from the first 11 months following tracer application (Jan 23/24, 2010 – Dec 27, 2010) are shown in Figure 2 and 3 (Pile 4 and 5, respectively). Initial breakthrough of bromide in Pile 4 was observed in all four lysimeters 4 to 6 hours following tracer application. Lysimeter B produced the highest concentrations at 1.3 g/L (or $C/C_o = 0.44$), 1.5 days following tracer release. Peak concentrations from Lysimeter A (located at the center of the pile base) were approximately one-third the concentration of Lysimeter B ($C/C_o = 0.15$). Trace bromide concentrations (i.e., $C/C_o = <0.005$) from Lysimeter C, not located vertically below the pile crown, suggest flow pathways have a minor horizontal component to a depth of 10 m. Tracer concentrations from Pile 4 decreased until the onset of the dry season in May, from which point lysimeters A, B and D showed similar steady, low concentrations (or $C/C_o = 0.001$). The onset of the 2010 – 2011 wet season coincided with low to negligible bromide concentrations from lysimeters A and D, but slightly higher concentrations in Lysimeter B ($C/C_o \leq 10^{-4}$. Lys A and D; $C/C_o \geq 10^{-3}$ (Lys B)) (Figure 2A-inset). These results suggest that lysimeters A and D were sufficiently flushed before the onset of the 2010 – 2011 wet season, indicating dominantly preferential flow. The results from Lysimeter B suggest a lower tracer percentage traveled along macropores, thereby producing concentrations up to an order of magnitude higher than those from lysimeters A and D 10 months following tracer application.

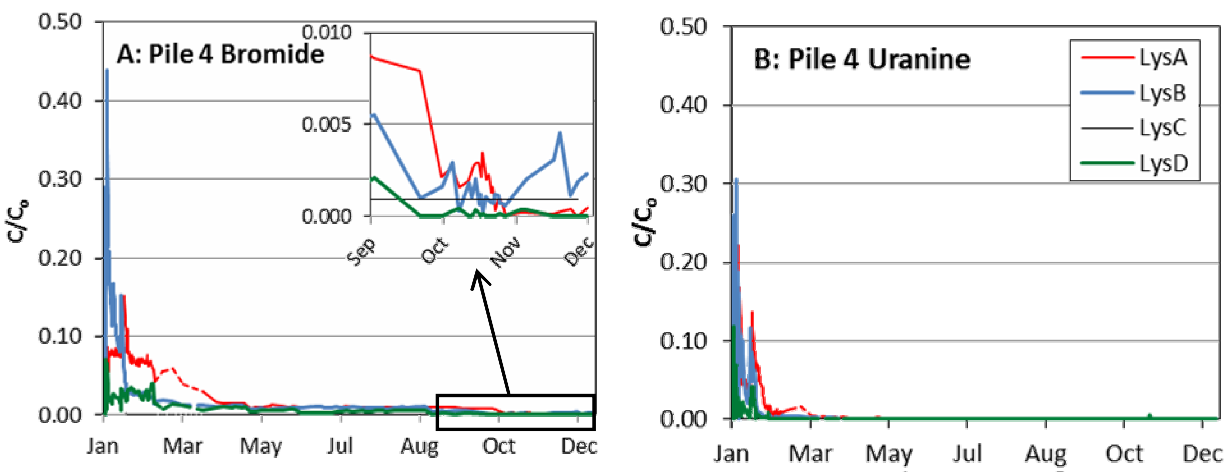

Figure 2. Pile 4 bromide and uranine breakthrough concentrations from January – December, 2010.

Uranine breakthrough curves from all four Pile 4 lysimeters are comparable to bromide results and uranine C/C_o values from the first 2 weeks are similar to those from the conservative (bromide) tracer analyses. Uranine is known to adsorb to material in moderate to long interaction times between infiltrating waters and waste-rock (Flury and Wai, 2003). The similarity in C/C_o values from bromide and uranine indicate little mixing/dilution occurred and confirm the tendency of flow along preferential pathways following rain events similar to the tracer application intensity/duration.

3.1.2 Pile 5 – Class A and C material

Tracer breakthrough from Pile 5 lysimeters occurred sporadically over a period of weeks, unlike Pile 4 which showed relatively uniform tracer breakthrough within hours of tracer application. The first breakthrough from Pile 5 occurred in Lysimeter D (i.e., $C/C_o = 3.5 \times 10^{-6}$) at four hours. However, sporadic and similarly low to negligible concentrations of bromide (i.e., $C/C_o < 10^{-4}$) were observed for two weeks before the tracer was detected continuously at concentrations greater than 0.1% of the applied concentration. The first occurrence of bromide at Lysimeter B occurred 48 hours following release (i.e., $C/C_o > 0.01$). Bromide breakthrough from Lysimeter A required twice the time and was 100 times lower than that in Lysimeter B (i.e., 4 days; $C/C_o \sim 10^{-4}$). Unlike Lysimeter D, bromide was released continuously following its first arrival at both Lysimeter A and B. Lysimeter C yielded bromide sporadically for approximately one month after application, before systematically releasing low to negligible bromide concentrations (i.e., $C/C_o < 10^{-4}$). To date, maximum C/C_o concentrations are considerably lower (≥ 10 times) than those observed from Pile 4. Negligible uranine has reached the base of Pile 5, with one uranine peak coincident with a bromide peak on Feb 2, 2010 (Figure 3). No flow trends can be ascertained from the first 11 months of uranine analyses, likely due to its adsorption to pile material and longer water-rock interaction times.

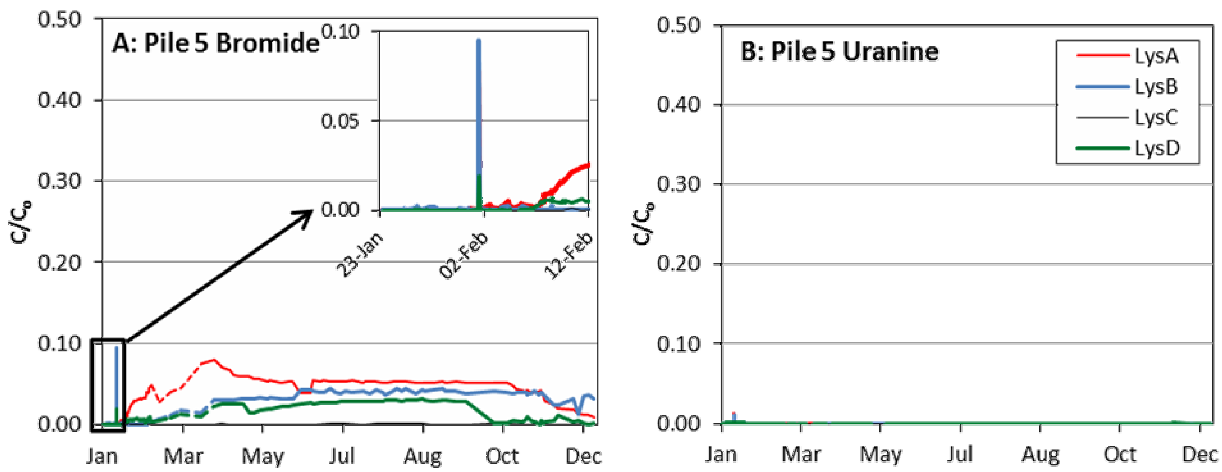

Figure 3. Pile 5 bromide and uranine breakthrough concentrations from January – December, 2010.

3.1.3 Daily flow characteristics

Tracer data is available through December 2010, however, flow response has been recorded from tipping buckets from Pile 4 and 5 lysimeters continuously since June 2009 (Figure 4A and B). Pile 4 sub-lysimeters respond within 1 day following large rain events (i.e., > 8 mm/d; Figure 4C). Pile 4 Lysimeter A and C respond similarly in timing and intensity, whereas Lysimeter B responds in timing, but not intensity. The waste-rock above Lysimeter B (in Pile 4) contains the highest amount of Class B material (refer to Figure 1), suggesting Class B facilitates channeling of infiltration as is observed with Class C material. However, the lower intensity suggests a significant proportion of infiltration does not follow these preferential flow paths, which was also noted in tracer results. Pile 5 has lower maximum daily flow rates (than Pile 4) and Lysimeters A and B respond much slower to large rain events, with lag times of 2 – 4 days. Lysimeter C, with the highest proportion of Class A material above it, has a muted response to rain events and a lower maximum daily flow rate. Comparison of these results with ratios of intrusive (Class A) to marble (Class C) material in Pile 5 indicates response is slower with increasing proportion of Class A (i.e., Lysimeter C > Lysimeter B > Lysimeter A, in decreasing response time).

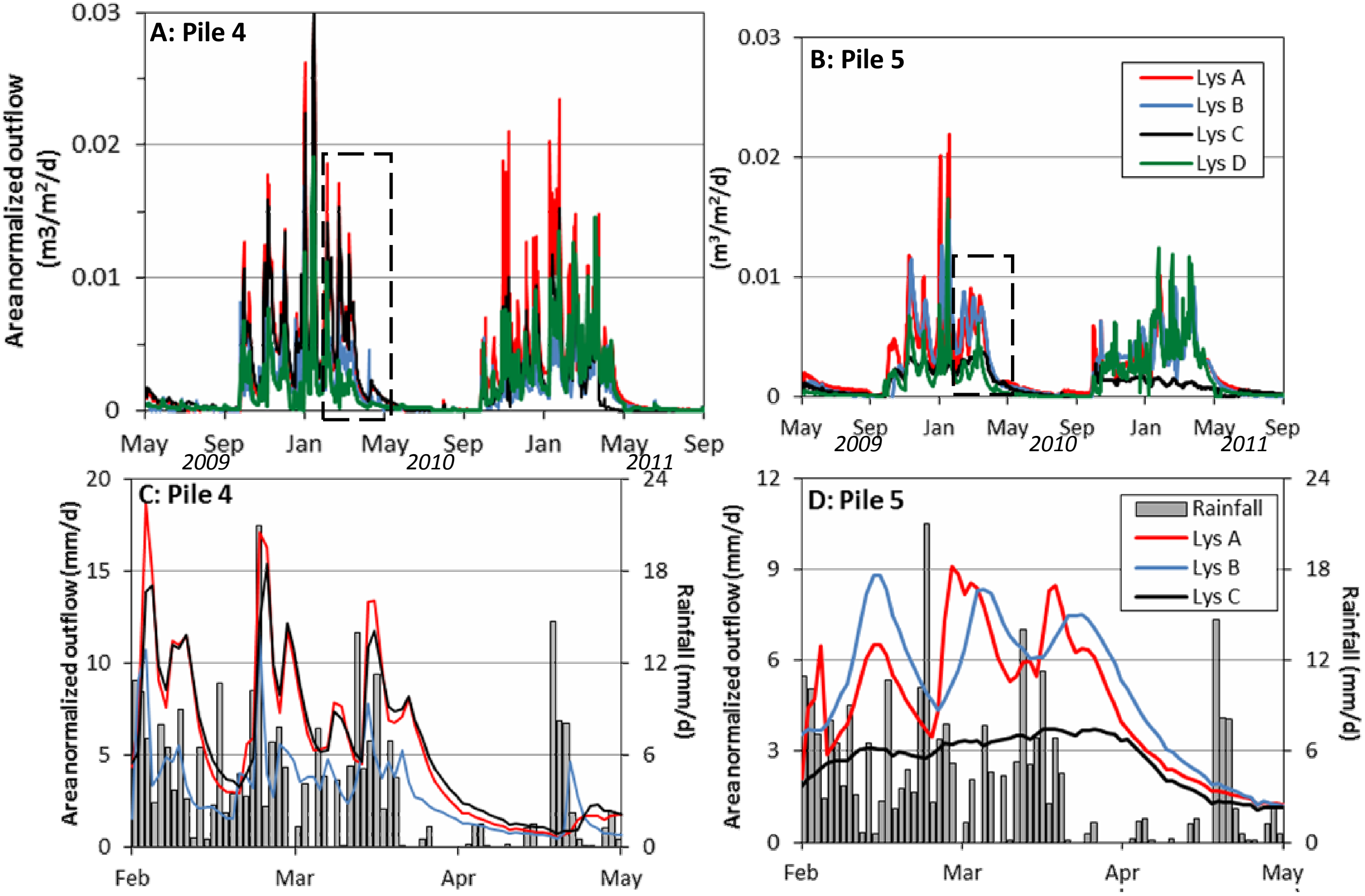

Figure 4. Daily flow rate from Pile 4 (A: Class B and C material) and Pile 5 (B: Class A and C material). Insets from both figures are shown in C and D, which detail lysimeter response following rainfall events.

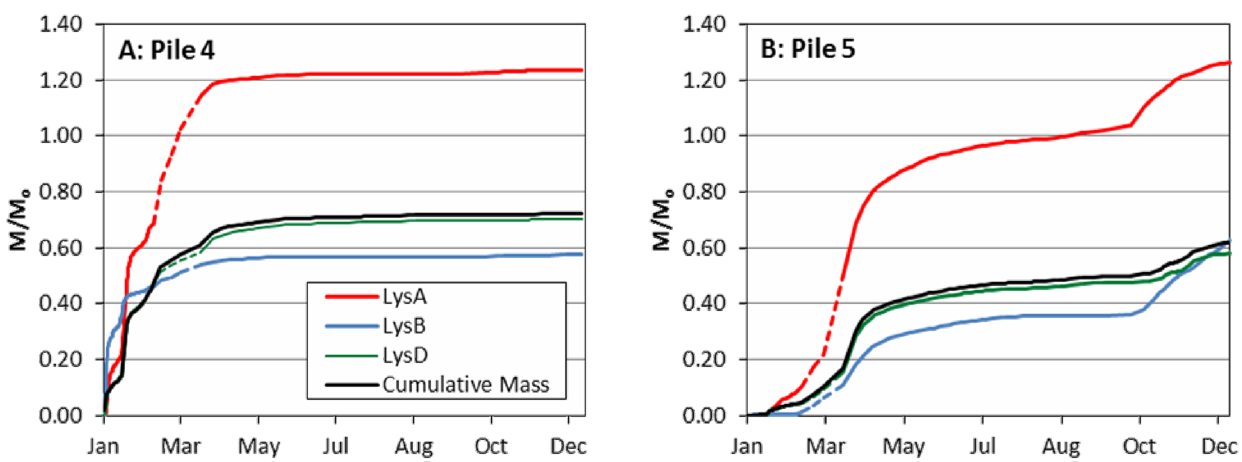

Figure 5. Cumulative mass release of bromide from Pile 4 and 5.

3.1.4 Tracer mass release trends

Mass released from lysimeters in Pile 4 and 5 is obtained by combining daily flow estimates with tracer concentrations (Figure 5A and B, respectively). Note that results from Lysimeter C are omitted from Figure 5 due to negligible mass release. Lysimeter A from both Pile 4 and 5 released over 100% of area normalized bromide mass (i.e., assuming vertical flow paths and uniform distribution) at 54 days and 221 days (respectively) following tracer study initiation. Two possible reasons exist for the observed surplus from this lysimeter. Firstly, the unsaturated hydraulic conductivity of Class C (i.e., $K(\theta)$) may be significantly higher than that of Class A or B. Class C is present in the highest proportion above Lysimeter A in Pile 4 and 5 (i.e., 75% and 92%, respectively) and may present more extensive channelling or preferential flow paths than the latter two material types. Additionally, the proportion of Class C to non-Class C material overlying Lysimeter B and D in both piles is similar, which likely contributes to the similarity of their tracer mass curves.

Secondly, the internal structure of each pile, in particular in Pile 5 which contains alternating fine-grained Class A with coarse-grained Class C materials, can contribute to a significant unsaturated hydraulic conductivity contrast (capillary breaks) between the end-dumped layers (Bussière et al, 2003). These characteristics, in addition to the pile geometry, may support unsaturated flow to preferentially follow the sloped layer interfaces. This may explain the large tracer mass recovered from Lysimeter A in Pile 5, which intersects the interface between Class A and Class C material (refer to Figure 1).

In the 11 months following the start of the tracer study, approximately 72% and 60% of the total tracer had been released from Pile 4 and 5; respectively. Fifty percent of the tracer applied to Pile 4 was recovered in one month following application, whereas Pile 5 lagged by over half a water year, with its cumulative tracer mass reaching 50% at the onset of the 2010 – 2011 wet season (i.e., October, 2010; ~ 10 months following application). Table 2 summarizes composition and flow details shown in the previous four figures.

Table 2. Summary of composition and flow characteristics from Pile 4 and 5 lysimeters.

	Pile 4				Pile 5			
	Lys A	Lys B	Lys C	Lys D	Lys A	Lys B	Lys C	Lys D
% B (P4) or A (P5)	25	40	0	25	8	28	40	44
% C	75	60	100	75	92	72	60	56
% of total discharge	2.9	1.6	2.8	92.7	2.7	2.5	1.3	93.5
Max Flow (m^3/d)	0.48	0.27	0.48	25	0.35	0.24	0.060	21
M_o (kg)*	1.22	1.22	0	23.2	1.31	1.31	0	22.8
Mass (kg)**	1.51	0.71	0.015	16.2	1.65	0.82	0.0077	13.2
t (d; for $M/M_o = 0.5$)	16	52	n/a	39	67	302	n/a	292

* Initial mass (M_o) determined from applied bromide concentration × applied volume × % applied area; sublysimeters represent a 16 m^2 area, and total tracer footprint dimensions (Lys D) are shown in Table 1.
** Bromide concentration × discharge volume.

The hydrologic response in Pile 4 and 5, as observed from tracer study results and daily flow estimates, indicate Class C rich regions report higher flow volumes than regions rich in Class A and B. Class B and C support predominantly preferential flow paths, as suggested by faster mass release in Pile 4 relative to Pile 5. Of Class B and C, the former presents higher C/C_o values initially, however regions with higher proportions of Class C result in a faster release of tracer mass overall. Class A material contributes much slower responses to rain events, with up to 5 times longer response times than those with lower Class A proportions. Class A material, unlike Class B and C material, yields more matrix-flow regimes.

3.2 Material characteristics

Previous studies by Smith and Beckie (2003) have shown the main factors controlling fluid flow and drainage chemistry are particle size distribution (PSD) and texture, as water retention generally increases as particle size and porosity decrease (Aubertin et al., 2003; Fala et al., 2005). Investigation of the physical properties of each material and the estimation of soil water characteristic curves were used to elucidate the basis of these flow differences.

PSD analyses conducted on fourteen samples of Antamina's waste-rock, with 4 – 5 tests per waste-rock class are shown in Figure 6A. Class B and C waste-rock is the coarsest, as denoted by the steepest PSD slope, and the latter shows the narrowest variation within each grain size fraction. The proportion of material passing the 2 mm sieve size can act as a qualifier for flow regimes. Specifically, samples containing greater than 20 % passing 2 mm present more 'soil-like' or matrix flow regimes, whereas samples with less than 20% passing this sieve size favour more 'rock-like' or preferential flow regimes (Smith and Beckie, 2003). Values from Class A, B and C are 23%, 6% and 4% (respectively), indicating the finer grained Class A material likely favours matrix flow regimes and the latter two classes favouring preferential flow.

To further evaluate the 'rock like' materials (Class B and C), PSD results were normalized to the amount of material passing the 4.75 mm diameter (Figure 6B). This mesh size was chosen as materials with diameters greater than 4.75 mm exhibit little capilliarity or ability to hold moisture, regardless of a dense or loose arrangement or texture (Aubertin et al., 2003). Class C waste has ~ 20 % less material (than Class B) passing sieve sizes between 2 mm and 0.074 mm, which is suggestive of a higher likelihood of preferential flow behaviour. Similarly, although Class B material shows steep PSD curves and low percentage passing the 2 mm sieve size, it is conceivable that a proportion of infiltration may be directed along slower matrix flow paths.

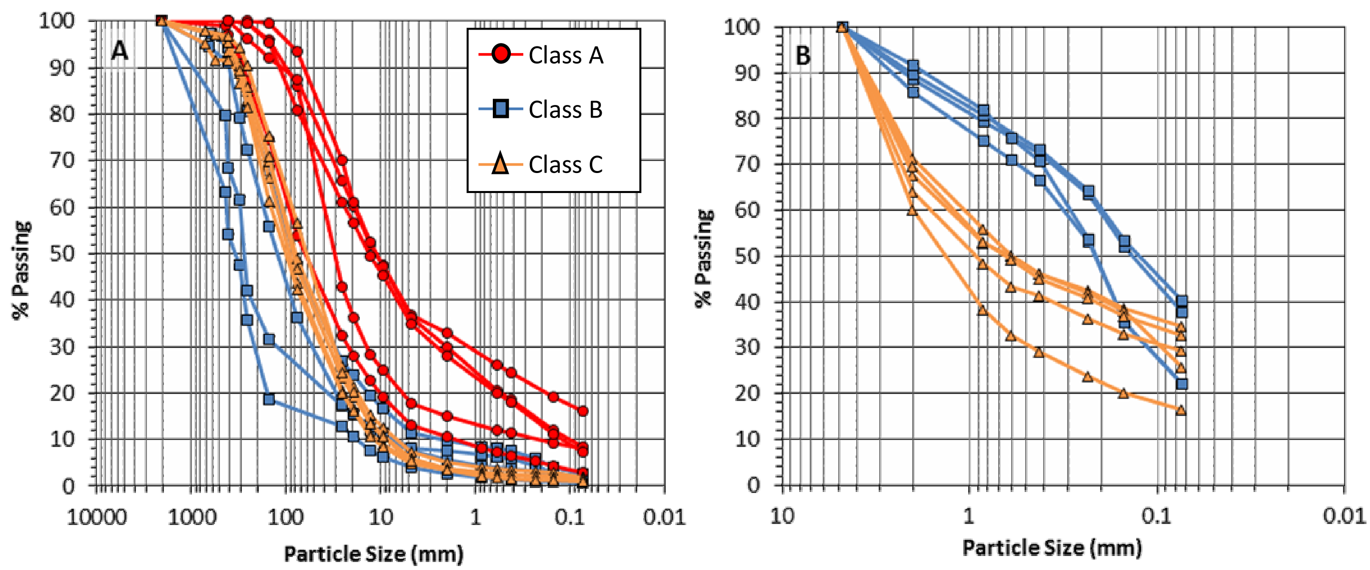

Figure 6. Particle size distributions from Antamina waste-rock material. A: All size fractions; B: Size fractions ≤ 4.75 mm, normalized to the percent passing the 4.75 mm sieve size.

Results from these PSD analyses were incorporated into SoilVision software, along with porosity, specific gravity and/or bulk density testing. Table 3 lists input parameters and modeled results (i.e., air-entry values and residual saturations). Figure 7 graphically displays soil water characteristic curves produced by SoilVision. Class A material has the highest air-entry and residual saturation values, which were up to 10 times higher than those from Class B and C. Modeled air-entry values were lower than the lowest Tempe cell pressure range (i.e., 1 kPa). The limited pressure range from the Tempe cell method restricts its effectiveness in characterizing the unsaturated behaviour of Antamina material, but results (not shown) did show similarly steep drainage curves and higher maximum volumetric water contents in Class A than Class B material, which is similar to results shown in Figure 7.

In large rainfall events, there is low matric suction and surface water enters larger pores (i.e., macropores), which have a higher hydraulic conductivity and are hydrologically effective at channelling water (Bevan and Germann, 1982; Bews et al., 1997; Birkholzer and Tsang, 1997). A low to no air-entry value can signify higher hydraulic conductivities in macropores, which can be attributed to continuity in the macropore-space and poor connectivity of macropores with remainder of the porous medium (Nichol, 2002). From model simulations, Class C material has the lowest air-entry values at 0.04 ± 0.01 kPa, followed closely by Class B material at 0.06 ± 0.03 kPa. The lysimeter with the highest proportion of Class C material in both piles was Lysimeter A, which released the highest proportion of tracer mass.

Table 3. Input parameters and results from modeled soil water characteristic curves.

Waste Class	Residual Water Content (%)	Dry Density (kg/m^3)	Specific Gravity (g/cm^3)	Porosity	Air-Entry Pressure (kPa)	Residual Saturation
A	0.03 – 0.06	1725 – 1770	2.65 – 2.67	0.33 – 0.35	0.29 ± 0.23	0.11 ± 0.03
B	0.04 – 0.07	1821 - 1846	2.53 – 2.56	0.28 – 0.31	0.06 ± 0.03	0.06 ± 0.02
C	0.06	1982	2.79	0.29	0.04 ± 0.01	0.02 ± 0.01

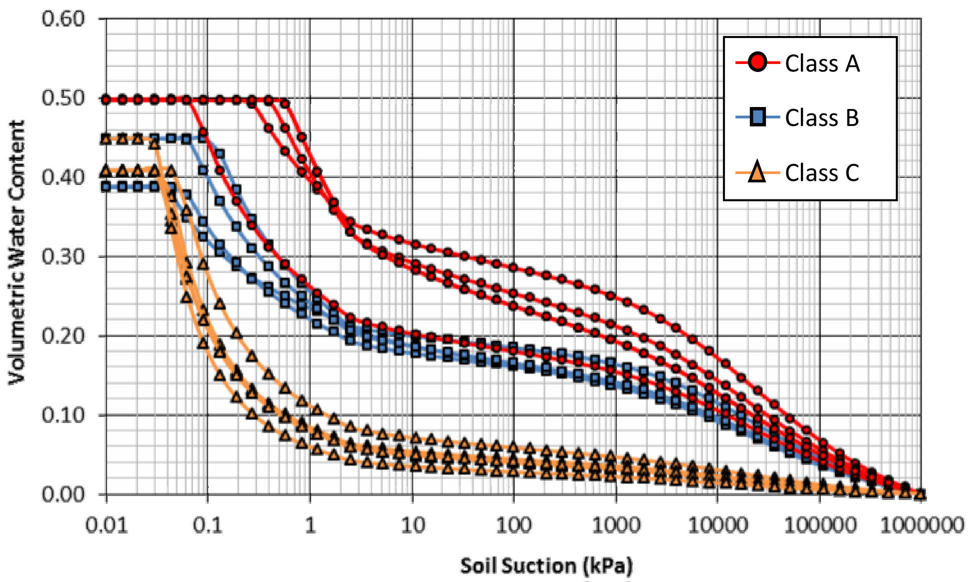

Figure 7. Modeled soil water characteristic curves of Antamina waste-rock.

At more moderate to lower infiltration events, there is higher matric suction and water is concentrated in the finer grained areas of material where it is held under capillary tension (Nichol, 2002). The tracer application is representative of a 4-year return period event, or a moderate rainfall event. The air-entry values of Class A material are up to 10 times greater than those from Class B, which are slightly higher than Class C. As such, the slower tracer release from Pile 4 and Pile 5 lysimeters underlying greater proportions of Class B or Class A (respectively, and in comparison to Class C) can be attributed to these material characteristics. Specifically, two trends can support this observation; firstly the continued tracer release from Pile 5 throughout the dry season indicates tracer is infiltrating a larger percentage of the finer (or matrix) pore space in Class A material and thereby released at significantly slower rates than Class B or C material. Secondly, tracer concentrations from Pile 4 Lysimeter B (with a 2:3 ratio of Class B to Class C) at the onset of the 2010-2011 wet season were 10 times higher than those Lysimeter A or D (both containing higher proportions of Class C). This result supports the previously described assessment that a proportion of tracer infiltrated the finer grained areas of Class B material and moves at a slower rate than the majority of the pore space.

4. Conclusions

Tracer study results, continued flow monitoring, and physical soil testing indicate the finer-grained Class A intrusive material is most likely to support matrix flow. The Class A intrusive material is described as 'soil-like', with 23% material having diameters < 2 mm and high air-entry values of ~ 0.11 kPa. Regions with high Class A proportions respond slower to infiltration events, have later breakthrough curves, lower concentrations and overall slower tracer recovery. These characteristics yield a dominantly matrix flow regime within Class A material. These results highlight the likelihood of longer interaction times between Class A waste-rock and infiltrating waters, which, in some circumstances, can be associated with higher solute loadings in drainage.

The coarser-grained Class B and Class C materials are described as 'rock-like' with only 6% and 4% (respectively) passing the 2 mm sieve diameter, and low air-entry values (i.e., ≤ 0.06 kPa). Regions of the test piles containing high proportions of Class B and C material respond quickly to rainfall events, show fast tracer breakthrough and high overall recovery. These characteristics indicate a large degree of interconnectedness in macropores in the porous medium and support a preferential flow regime. In addition to preferential flow, Class B material also shows evidence of slower flow regimes; it has a higher percentage of the finer grain size fractions (than Class C) and yielded higher tracer concentrations over longer time durations. Shorter water-rock interaction times characteristic of preferential flowpaths, in addition to the lower overall metal-sulphide percentages defining Class B and C waste-rock, suggests there is a lower potential for high dissolved metal concentrations in drainage.

These results can be extrapolated to large-scale waste dumps at the Antamina mine. Specifically, the East Dump, which receives Class A material and lesser amounts of Class C material and is compositionally similar to Pile 5 of this study (i.e., also received Class A and C material), will likely display a matrix-dominated flow regime and slow response times to infiltration events. However, large textural differences between these two waste rock classes increases the likelihood of infiltrating waters following end-dumped slope faces and decrease overall water-rock interaction times. Equally, it is plausible that the flow regime in Antamina's Tucush Dump, which receives Class B and C material and is compositionally comparable to Pile 4, will support a higher component of preferential flow than observed in the East Dump. As such, this study and the results therein can provide insights into large dump behaviour and can aid in operational decisions about waste mixing and segregation at the site.

Acknowledgements
The authors wish to thank Antamina, Teck, and NSERC for the funding this project. Special recognition is directed to Fabiola Sifuentes, Bevin Harrison, Celedonio Aranda, Edsael Sanchez Rondan and Janeth Vizconde of Antamina for their generous amount of time and assistance to this project. Also, to Michael Gupton and Holly Peterson, whose proficiency in tracer experiments, made this study a success.

References

Aubertin, M., Mbonimpa, M., Bussière, B., and Chapius, R. (2003) A model to predict the water retention curve from basic geotechnical properties. Canadian Geotechnical Journal, Vol. 40(vi), pp 1104-1122.

Bay, D.S. (2009) Hydrological and hydrogeochemical characteristics of neutral drainage from a waste-rock test pile. *Master's Thesis.* University of British Columbia, Vancouver, BC. 331 p.

Bay, D., Peterson, H., Singurindy, O., Aranda, C., Dockrey, J., Sifuentes, F., Mayer, U., Smith, L., Klein, B. and R. Beckie. (2009) Assessment of neutral pH drainage from three experimental waste-rock piles at the

Antamina mine, Peru. In, Proceedings of the 8th International Conference on Acid Rock Drainage, June 23-26, 2009 Skellefteå, Sweden.
Bevan, K. and Germann, P. (1982) Water flow in soil macropores. Water Resources Research, Vol.18(v), pp. 1311-1325.
Bews, B.E., O'Kane, M.A., Wilson, G.W., Williams, D., and Currey, N. (1997) The design of a low flex cover system, including lysimeters for acid generating waste-rock in semi-arid environments. In, Proceedings of the 4th International Conference on Acid Rock Drainage. May 31-Jun 6, 1997, Vancouver, BC, Canada.
Birkholzer, J. and Tsang, C. (1997) Solute channelling in unsaturated heterogeneous porous media. Water Resources Research, Vol. 33(x), pp. 2221-2238.
Brussiere, B., Aubertin, M., and Chapuis, R.A. (2003) The behaviour of inclined covers used as oxygen barriers. Canadian Geotechnical Journal, Vol. 30(iii), pp. 512-535.
Christensen, J.E. (1942) *Irrigation by Sprinkling.* California Agriculture Experiment Station, Bulletin 670. University of California, Berkley p. 181-202.
Fala, O., Molson, J., Aubertin, M. and B. Bussière. (2005) Numerical modeling of flow and capillary barrier effects in unsaturated waste-rock piles. Mine water and the environment, Vol. 24, pp. 172-185.
Flury, M. and Wai, N.N. (2003) Dyes as tracers for vadose zone hydrology. Reviews of Geophysics, Vol. 41(i), 37p.
Fredlund, D.D., Fredlund, M.G., and Wilson, G.W. (1997) Prediction of the soil-water characteristic curve from grain-size distribution and volume-mass properties. In, The 3rd Brazilian Symposium on Unsaturated Soils. April 22 -25, 1997. Rio de Janeiro, Brazil.
Fredlund, D., & Xing, A. (1994) Equations for the Soil-Water Characteristic Curve. Canadian Geotechnical Journal, Vol. 31 , pp. 521-532.
Golder (1999) *Hydrology Design Parameters for Antamina Mine Tailings Facility, Antamina Project.* Technical Memorandum TM-6, Version 3. July 30, 1999. 192p.
Golder (2004) *Waste-rock Geochemistry – Phase 2, Antamina Mine, Peru.* Version 4.0. December 2004. 341 p.
Golder. (2010). *Waste-rock and Tailings Geochemistry – Field Cell Monitoring, Dec 2002 to May 2009.* January 2010, 125 p.
Hirsche, T, Beckie, R., Mayer, K.U., Conlan, M., Klein, B., Smith, L., Blackmore, S., Peterson, H., Aranda, C. (2012) A field cell and humidity cell study of Mo and Zn attenuation by waste-rock mixing in neutral drainage conditions as a part of the Antamina Waste-rock Project, Peru. In, Proceedings of the 9th International Conference on Acid Rock Drainage (ICARD), May 20-26, 2012, Ottawa, Ontario, Canada
Nichol, C. (2002) Transient flow and transport in unsaturated heterogeneous media: Field experiments in mine waste-rock. *Ph.D dissertation.* University of British Columbia, Vancouver, BC.
Nichol, C., Smith, L., and Beckie, R. (2005) Field-scale experiments of unsaturated flow and solute transport in a heterogeneous porous medium. Water Resources Research, Vol. 41, 11p.
Presley, B.J. (1971) Appendix: Techniques for Analyzing Interstitial Water Samples. Part I : Determination of Selected Minor and Major Inorganic Constituents. *Initial Reports of Deep Sea Drilling Project, Volume II.* U.S. Government Printing Office. Washington, D.C.
Smith, L. and Beckie, R. (2003) Hydrological and geochemical transport processes in mine waste-rock. *Environmental Aspects of Mine Wastes. Short Course Series v.31.* Mineralogical Association of Canada.
Soil Moisture, Corp. (1995) 1400/1405 Tempe pressure cell operating instructions, Viewed 19 September, 2011 http://www.soilmoisture.com/pdf/14001405.pdf
Sracek, O., Choquette, M., Gélinas, P., Lefebvre, R., Nicholson, R.V. (2004) Geochemical characterization of acid mine drainage from a waste-rock pile, Mine Doyon, Québec, Canada. Journal of Contaminant Hydrology, Vol. 69, pp. 45-71.